

# A Light and Electron Microscopic Analysis of Gentamicin Nephrotoxicity in Rats

Donald C. Houghton, MD, Michael Hartnett, MD,  
Mark Campbell-Boswell, BS, George Porter, MD,  
and William Bennett, MD

The sequence of proximal tubular damage and repair after gentamicin sulfate administration was studied by light and electron microscopy in Fischer 344 rats. The drug was administered at a dose of 40 mg/kg for up to 14 days. Although epithelial destruction was progressive with time, the extent and degree of tubular damage varied among animals at each interval. Tubule regeneration began to occur by the tenth day despite continued drug administration. Regenerating cells appeared to originate from residual epithelial cells in areas of tubular damage. The morphologically immature regenerating cells are apparently metabolically immature as well and appear not to be susceptible to toxic effects of the drug. Tubules were repopulated by 3 days following cessation of gentamicin administration. Except for foci of tubular atrophy and interstitial fibrosis, cortical tissues were comparable to controls ultrastructurally at the end of 31 days. (*Am J Pathol* 82:589-612, 1976)

SINCE AMINOGLYCOSIDE ANTIBIOTICS are known to be nephrotoxic in animals and man, renal dysfunction was anticipated when gentamicin was first made available for clinical use.<sup>1,2</sup> Gentamicin renal toxicity has been reported to be relatively infrequent,<sup>2,3</sup> although estimation of clinical incidence has been obscured by the setting in which the drug is given, i.e., serious sepsis, and by the insensitivity of parameters to monitor toxicity in patients.<sup>1,4,5</sup> Generalizations on relative toxicities between various aminoglycosides, based on animal studies, have been difficult in view of marked variability in development of nephrotoxicity among different species of experimental animals.<sup>1,5,6</sup> For example, in some strains of rat, gentamicin administered in amounts far exceeding the usual human therapeutic doses failed to induce renal disease.<sup>6-9</sup> Yet Kosek *et al.* have recently demonstrated light and electron microscopic evidence of proximal tubular damage in Fischer rats given gentamicin in doses comparable to those used clinically.<sup>10</sup> In that morphologic study, they showed that pathologic changes were a function of the daily dose of gentamicin. Using a similar model we have studied the sequence of damage and repair that occurs in the proximal tubules of rat kidneys during and following administration of gentamicin in a fixed daily dose for up to 14 days.

---

From the Departments of Pathology and Medicine, University of Oregon Health Sciences Center and the Veterans Administration Hospital, Portland, Oregon.

Accepted for publication November 24, 1975.

Address reprint requests to Dr. Donald C. Houghton, Department of Pathology, University of Oregon Health Sciences Center, Portland, OR 97201.

## Materials and Methods

Experiments were performed on 4- to 6-week-old Fischer 344 rats weighing between 175 and 300 g each. All animals were housed in cages in groups of 3 and were fed standard rat chow and given tap water to drink *ad libitum*. Two weeks were allowed before the start of any experiment to permit the animals to adjust to this environment. Blood was obtained at intervals by tail tip amputation and at the end of sacrifice by needle aspiration of the inferior vena cava. Blood urea nitrogen (BUN) and serum creatinine determinations were made by autoanalyzer techniques adapted for use on small blood samples. The technique was validated by blind parallel assay of specimens using quantitative methods and by assaying solutions prepared with known amounts of exogenous urea and creatinine.

Gentamicin sulfate was administered at a dose of 40 mg/kg/day with all injections being diluted to a volume of 1 cu cm with normal saline and administered in two divided subcutaneous doses. Groups of rats received 7, 10, 12, and 14 days of gentamicin and were sacrificed approximately 15 hours after the last dose. In addition, other groups of rats were given 10 days of gentamicin and sacrificed 1, 2, 3, 7, and 31 days after the last dose. A 10-day treatment period was chosen because it reliably produced both reversible azotemia and extensive ultrastructural damage. Control histology and chemistry values were obtained from rats which were sacrificed without prior treatment or after re-receiving 1 cu cm of normal saline twice a day for each experimental interval up to 14 days. Baseline BUN and creatinine levels were drawn from most animals prior to the beginning of an experiment.

At the termination of the experiment, animals were anesthetized with ether, and a ventral midline abdominal incision was made to expose the abdominal contents. Following exsanguination via venipuncture of the inferior vena cava, the incision was extended superiorly to expose the thoracic contents. The left ventricle was then punctured, and the systemic vasculature perfused for several minutes with Krebs-Ringer solution. The pedicle of one kidney was then clamped, and the kidney was removed, sliced, and fixed in Bouin's solution for light microscopy. The remaining kidney was fixed for electron microscopy *in situ* by cardiac perfusion with 1% glutaraldehyde in 0.1 M phosphate buffer. Perfusion solutions were buffered at pH 7.4 to 7.5 and had osmolalities of approximately 300 mOsmoles. After 5 minutes of perfusion with fixative, pieces of renal cortex were excised and immersed for an additional 2 hours in the same fixative. Tissue cut in 1-cu mm blocks was postfixed for 2 hours in 2% osmium tetroxide in 3% sucrose and 0.05 M cacodylate buffer, pH 7.4. Tissue blocks were rapidly dehydrated in graded ethanol solutions, embedded in Araldite 502 according to the procedure of Luft,<sup>11</sup> and sectioned with glass knives on a Porter-Blum MT2-B ultramicrotome or LKB ultratome. Thin sections stained with uranyl acetate and lead citrate<sup>12</sup> were examined at 60 kV in a Phillips EM-200 electron microscope. One-micron-thick sections of Araldite-embedded tissue, stained with toluidine blue, were also examined by light microscopy.

## Results

### Treatment Period

The mean BUN and serum creatinine values at the end of each treatment period from 7 to 14 days are presented in Table 1. Because there were no significant differences between baseline and control chemistries, these were combined.

By the end of the first week of gentamicin administration, there was little change in BUN and creatinine levels, but after 10 days there were significant elevations and, with successive treatment intervals, progressive

Table 1—Blood Urea Nitrogen and Serum Creatinine Levels in Rats During Gentamicin Administration

Duration of gentamicin administration	N	Mean BUN (mg%) (range)	Mean serum creatinine (mg%) (range)
Baseline & controls	46	22 (18-29)	0.6 (0.3-1.0)
7 days	24	26 (18-32)	1.0 (0.6-1.7)
10 days	12	66 (38-145)	2.9 (1.0-7.7)
12 days	9	108 (43-170)	3.9 (1.8-9.0)
14 days	8	119 (35-170)	6.7 (1.0-13.1)

uremia. There were marked differences in severity of renal dysfunction among animals in each group.

Light and electron microscopic appearances of kidney tissues from control rats were in accordance with descriptions by Rouille<sup>13</sup> and by Ericsson and Trump<sup>14</sup> (Figures 1 and 2).

After 7 days of continuous gentamicin administration, the light microscopic alterations of the kidney were minimal. There was vacuolization of proximal tubular epithelium in the superficial cortex. Nuclei of most proximal tubular cells were enlarged and contained prominent central areas of clumped chromatin. Mitoses were rare. The ultrastructure of the proximal convoluted tubules differed from controls in several ways (Figure 4). Most epithelial cells contained increased numbers of large, irregular, dense lysosomes, predominantly cytosomes and cytosegosomes.<sup>10,14</sup> Within many of these structures were numerous unicentric and multicentric myeloid bodies (Figure 5). Occasionally myeloid bodies appeared in the cytoplasm without surrounding lysosome membranes, and they were sometimes present in small, tightly packed aggregates in the lumina of the proximal tubules. Mitochondria were swollen; many were rounded in comparison with controls. Vacuoles, some quite large, had appeared predominantly in the basal half of the cells. The cisternae of the rough endoplasmic reticulum were markedly dilated.

In the 1- $\mu$  Araldite-embedded tissue sections, lysosomes appeared as small, rounded or irregular, darkly staining cellular inclusions (Figure 3). Myeloid bodies were apparent as tiny dots or granules within the lysosomes or within tubular lumina. Glomeruli, the distal convoluted tubules, and cortical collecting tubules appeared normal by both light and electron microscopic examination.

After 10 days of gentamicin administration, there was much more extensive damage by light microscopy (Figures 10 and 11). In the superficial cortex there were patchy proximal tubular epithelial necrosis and desquamation. The extent of tubular necrosis varied from one animal

to another, but in most cases the epithelium of about half of the proximal tubules in the outer cortex was destroyed. Many epithelial cells were vacuolated and appeared to be undergoing granular disintegration. On electron microscopic examination, tubules with minimally altered epithelium were found side by side with those having severely disrupted or sloughed epithelium (Figure 7). In the severely disrupted tubules, remnants of tubular cells consisted of cytoplasmic collections of disorganized, severely damaged organelles (Figure 6). At times these cells appeared to be only tenuously attached to the basement membrane. Mitochondria were markedly swollen, with attenuated and distorted cristae and loss of matrix; some were disrupted altogether. Myeloid bodies were quite numerous in some areas, but in general, lysosomes and myeloid bodies were less conspicuous in all cells at 10 days than they were at 7 days.

Cells in intermediate stages of damage exhibited varying degrees of mitochondrial swelling and destruction, vacuolization of cytoplasm, simplification and loss of basal membrane infoldings, and disarray of microvillous borders. Many tubules, both proximal and distal, were filled with brightly eosinophilic, granular material which by electron microscopy consisted of cytoplasmic debris including numerous myeloid bodies.

In some tubules where epithelial desquamation had occurred, squamoid cells, almost imperceptible by light microscopy, covered or partially covered the basement membranes. By electron microscopy, they were relatively undamaged cells of two types (Figures 8, 9, and 12). Cells of one type were apparently residual from the original epithelial population. These cells had well-developed microvillous borders and compact cytoplasmic matrices. They had small ovoid or cylindrical mitochondria, occasionally prominent smooth endoplasmic reticulum, and a few large lysosomes, some containing myeloid bodies. Basal infoldings were usually absent, and there were relatively few apical vesicles.

Cells of the second type, apparently regenerating cells, were comparatively much less differentiated. They were often taller with more loosely arranged cytoplasm containing large numbers of ribosomes. They had a few small round mitochondria and lysosomes which in some cases contained myeloid bodies. Microvilli were rudimentary or sometimes lacking altogether. Basal infoldings and apical vesicles were absent. Intermediate cells sharing features with each type were also noted. Where cells of either kind were flattened against otherwise denuded basement membranes they had distinctive undulating basal cell membranes which contacted the basement membrane at intervals. Occasionally these cells overlapped one another and insinuated themselves between damaged

cells and the basement membrane (Figure 8). Where the tubules were still relatively cellular, residual and regenerating cells were cuboidal. Collections of granular debris had been trapped between layers of the proximal tubular basement membranes. Epithelia of the pars recta, distal convoluted tubules, and cortical collecting tubules contained scattered dense lysosomes with myeloid bodies, but they remained intact.

After 12 days of drug administration, the difference in degree of proximal tubular damage from one animal to another was pronounced. In most animals, substantially more than half of the tubules of the outer cortex were undergoing necrosis (Figure 13). Many were clear or partially cleared of debris.

Ultrastructural damage of epithelial cells was severe. Some tubules were devoid of epithelium, but many were lined by flattened epithelium composed predominantly of regenerating cells. Mitotic figures were more numerous in epithelial cells at all levels of the proximal tubules.

In some animals tubular disruption was still quite early. Tubules were packed with debris and evidence of reepithelialization was generally lacking.

In proximal tubules with intact residual epithelium, cells were vacuolated with fragmented coarsely granular cytoplasm, irregular luminal edges, and obscured brush borders. By electron microscopy the mild degree of damage in many of these cells was more typical of lesions of the 7-day stage.

Some cells of the distal convoluted tubules and cortical collecting tubules contained small numbers of dark irregular lysosomes and myeloid bodies. Glomeruli exhibited no abnormalities except for scattered collections of cell debris in the urinary space. Other than occasional short segments of severe cellular damage, the partes rectae of the proximal tubules were intact and showed mild alterations. Some of these epithelial cells contained large lysosomes, sometimes packed with multicentric myeloid bodies. They exhibited a spectrum of mitochondrial damage.

By 14 days, alteration of the epithelium of proximal convoluted tubules was nearly total. Tubules were nearly cleared of debris in most animals, although here again there was considerable variation. Regeneration was extensive (Figure 14). Basophilic epithelial cells without brush borders were taller than previously observed. Mitotic figures were numerous. There were occasional microfocal areas of necrosis in the partes rectae of the proximal tubules and in distal convoluted tubules. Lymphoid aggregates were distributed rather diffusely through the cortical and corticomedullary interstitium. Electron microscopically, while all stages of cellular change were represented, most tubules were lined by regen-

erating epithelium which was more differentiated than after 10 or 12 days of gentamicin. These cells were developing short microvilli, increased numbers of mitochondria, smooth endoplasmic reticulum, and rudimentary basal unfoldings. There were focal areas of extreme wrinkling and thickening of basement membranes (Figure 15). Regenerating cells were laying down new layers of basal lamina and collections of debris were often trapped beneath the layers.

#### Recovery Period

Table 2 presents the mean BUN and serum creatinine levels in rats during the recovery periods after 10 days of gentamicin. While the numbers of observations after most intervals were small, there was an apparent steady improvement in blood chemistries during the first week of recovery which leveled off during the second week. The BUNs and creatinines remained slightly elevated as compared to controls and baseline values in the 2 animals studied at the end of 31 days of recovery.

A 24-hour delay of the sacrifice of animals after 10 days of gentamicin administration resulted in no appreciable difference in the light or electron microscopic appearances of the proximal tubules.

Significant change in the appearances of proximal tubules was first noticeable in animals examined 2 days after the last injection. Mitotic figures were more numerous at all levels of the proximal tubules and were occasionally identified in distal convoluted tubules and cortical collecting tubules. Most proximal and distal tubules were cleared of debris. Roughly half of previously denuded basement membranes were lined by low basophilic regenerating epithelium. The cells of a few tubules, apparently residual cells, had regained normal height and appeared normal electron microscopically, except that they lacked basal infoldings (Figure 16).

By 3 days after the last injection, most tubules were lined by low

Table 2—BUN and Serum Creatinine Levels During Recovery After Ten Days of Gentamicin Administration

Interval between last dose of gentamicin and sacrifice (days)	N	Mean BUN (mg%) (range)	Mean serum creatinine (mg%) (range)
1	3	83 (55-115)	2.2 (1.2-3.1)
2	2	79 (44 & 113)	2.0 (1.1 & 2.9)
3	3	66 (30-119)	1.8 (0.9-3.3)
7	11	49 (24-183)	1.4 (1.0-2.4)
14	2*	32 (30 & 34)	1.0 (0.8 & 1.2)
31	2*	36 (34 & 38)	1.5 (1.4 & 1.6)

\* One rat died 10 days after the last injection.

basophilic epithelium (Figure 17). Other tubules were composed of tall vacuolated eosinophilic residual cells. Tortuous groups of intertwined tubules with basophilic regenerating epithelia and numerous mitotic figures extended from the corticomedullary areas into the superficial cortex.

By 7 days after the final dose, regenerating proximal tubular epithelial cells were regaining normal height and structure (Figures 18 and 21). They had dense, well-developed microvilli and simple short basal infoldings. In a few areas, regeneration was less advanced; cells were lower with few organelles and rudimentary microvilli. Myeloid bodies were found at the apices of some cells, apparently being extruded into the lumina (Figure 19). Small collections of debris in the tubular lumina consisted predominantly of myeloid bodies (Figure 20). Foci of regeneration were occasionally encountered in distal convoluted tubules and in cortical collecting tubules.

After 4 weeks of recovery, most areas of the kidney were comparable to controls by light and electron microscopy (Figure 25). There were still occasional mitotic figures. In some areas there was prominent residual scarring. There were small subcapsular and deeper cortical scars containing collections of collapsed atrophic tubules (Figures 22 and 23). Ultrastructurally these tubules were composed of cells which were essentially undifferentiated (Figure 24). They had rudimentary microvilli and lacked basal infoldings. Cytoplasm was condensed, containing scattered unoriented mitochondria, small lysosomes, and relatively small numbers of ribosomes. In these areas the basement membrane showed the most extensive change. There were marked wrinkling and irregular thickening with multiple layering and focal areas of attenuation. Numerous collections of debris were apparently trapped among layers of the basement membrane.

## Discussion

Gentamicin, a widely used aminoglycoside antibiotic, is known to cause tubular necrosis in experimental animals.<sup>9,10</sup> In our study, proximal tubular destruction was progressive and nearly total by 14 days. The epithelium of the pars convoluta was most sensitive, displaying earliest and most persistent alterations. The extreme variation in degree and extent of renal damage was reflected by the wide ranges in the levels of BUN and serum creatinine among animals at every interval. Regeneration of tubular epithelia had begun by 10 days and, despite continued administration of the gentamicin, was progressing at 14 days. This may reflect a degree of protection that regenerating cells have from the toxic effects of gentamicin because of metabolic and functional immaturity.

Although the rats were still azotemic, regeneration of proximal tubular epithelium was nearly complete by 7 days after discontinuation of a 10-day course of gentamicin. Over the next 3 weeks, maturation of the regenerated epithelium occurred while the BUN and creatinine levels continued to fall. These findings are comparable to those from other studies of renal proximal tubular regeneration.<sup>15-17</sup> The source of the regenerating tubular cells is of interest. Our examination indicates that regenerating cells probably arise initially by progressive simplification and dedifferentiation of residual cells within areas of tubular necrosis. Residual cells were found at all levels of the disrupted proximal tubules, often in the presence of regenerating cells and apparent intermediate forms. By light microscopy, there was no evidence that repopulation of the tubular epithelium progressed from any particular part of the tubule. Mitoses were present at all levels of the cortex in even distribution. Similar patterns of tubular regeneration have been described by Oliver,<sup>18,19</sup> Cuppage and Tate,<sup>17</sup> Siegel and Bulger,<sup>20</sup> and Cuppage and Chiga.<sup>21</sup>

Thirty-one days after the discontinuation of gentamicin administration, BUN and creatinine levels had not returned to control values; this correlated with the residual microscopic damage. This residual damage consisted of interstitial fibrosis and tubular atrophy. Electron microscopically, the epithelial cells in these tubules had apparently failed to mature. Several authors have emphasized the importance of the basement membrane for proper maturation of the regenerating nephron and have concluded that tubular interstitial disease persisting after tubular necrosis was a result of severe damage or disruption of tubular basement membranes in both experimental<sup>16,18,20,21</sup> and clinical<sup>22</sup> settings. In our material, basement membrane distortion and thickening were most pronounced in tubules where epithelial regeneration was incomplete.

The basic mechanism underlying gentamicin-induced proximal tubular necrosis is unknown. Transport kinetics of the drug in proximal tubule cells have not been examined. The apparent distal progression of necrosis and patchy uneven nature of the tubular damage suggest a variable susceptibility of superficial cortical proximal tubules.

The pathologic significance of the increased numbers of large cytosomes and cytosegosomes in the proximal tubular epithelial cells after gentamicin administration and their relationship to the cytotoxic effects of the drug are speculative. These lysosomal structures are probably autophagic vacuoles resulting from sequestration of cytoplasmic fragments, membranes and organelles for lysosomal digestion.<sup>23</sup> While this phenomenon occurs to some extent in the process of normal cell metabolism, particularly in the rat proximal tubule,<sup>23</sup> acceleration of the rate of autophagy may occur after focal cell injury induced by toxins or



other adverse conditions.<sup>23,24</sup> An attractive possibility is that gentamicin-induced focal cytoplasmic injury results in an increased rate of autophagic activity in the proximal tubular cells.

The specific origin and significance of myeloid bodies are similarly not known. Although they can be induced in the cells of many tissues of experimental animals by drug therapy,<sup>25-27</sup> similar concentrically whorled membranous figures form spontaneously when certain lipids and mixtures of lipids, particularly phospholipids, are allowed to aggregate in water.<sup>28,29</sup> Myeloid bodies, then, may occur when the lipid constituents of the cellular lysosomes are altered, hydrated, or concentrated sufficiently to form membranous aggregates.<sup>10,27</sup> Hruban<sup>26</sup> has proposed that myeloid bodies occur as a result of inadequate or protracted degradation of membranes, primarily smooth endoplasmic reticulum, in autophagic vacuoles. He suggests that a prolonged state of degradation may occur when cytoplasmic membranes are heavily drug bound or when there is inhibition of the formation or function of autophagic vacuoles caused, for example, by inadequate lysosomal enzyme synthesis or inhibition of fusion of primary lysosomes with autophagic vacuoles. Earlier, the same author<sup>25</sup> observed that myeloid bodies occurred most consistently when protein and lipid synthetic processes were impaired. This is interesting in view of the ability of gentamicin to impair protein synthesis in bacterial systems.<sup>30</sup>

It is tempting to speculate that as a protective mechanism, the cell isolates and subsequently ejects gentamicin-injured or possibly gentamicin-bound cytoplasmic structures in the form of myeloid bodies. Similar mechanisms of lysosomal isolation or exclusion of toxic substances have been previously hypothesized.<sup>27,31</sup> In support of this possible mechanism is the observation in this study of myeloid bodies in the urinary space early, before cellular disruption is otherwise identified, and later, after it had apparently stopped in the 7-day regeneration rats. The accumulation of myeloid body-containing lysosomes was observed by Kosek<sup>10</sup> in rats receiving low, apparently nontoxic, doses of gentamicin. Presumably, cellular damage would become irreversible after such a mechanism to deal with the increasing cytoplasmic levels of gentamicin and its effects was overloaded. Whatever the cause for the lysosomal abnormalities, including the myeloid bodies, after gentamicin administration, their relationship to the toxic effects of the drug is yet to be determined.

## References

1. Falco FG, Smith HM, Arcieri GM: Nephrotoxicity of aminoglycosides and gentamicin. *J Infect Dis* 119:406-409, 1969
2. Jackson GG: Current therapeutics. CCXXXIV. Gentamicin. *Practitioner* 198:855-866, 1967

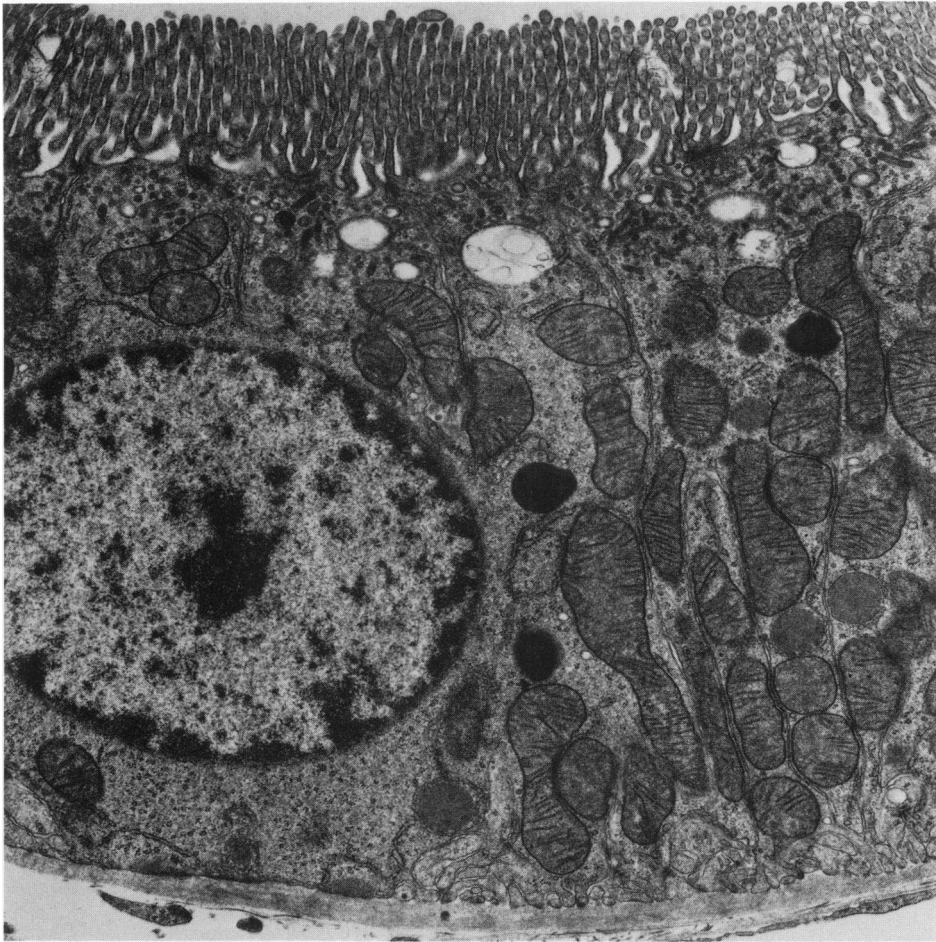
3. Abramowicz M, Edelmann CM Jr: Nephrotoxicity of anti-infective drugs. *Clin Pediat* 7:389-390, 1968
4. Wilfert JN, Burke JP, Bloomer HA, Smith CB: Renal insufficiency associated with gentamicin therapy. *J Infect Dis* 124(Suppl)S148-S155, 1971
5. Milman N: Renal failure associated with gentamicin therapy. *Acta Med Scand* 196:87-91, 1974
6. Black J, Calesnick B, Williams D, Weinstein MJ: Pharmacology of gentamicin, a new broad-spectrum antibiotic. *Antimicrob Agents Chemother* 3:138-147, 1963
7. Fillastre JP, Laumonier R, Humbert G, Dubois D, Metayer J, Delpech A, Leroy J, Robert M: Acute renal failure associated with combined gentamicin and cephalothin therapy. *Br Med J* 2:396-397, 1973
8. Lawson DH, Macadam RF, Singh H, Gavras H, Hartz S, Turnbull D, Linton AL: Effect of furosemide on antibiotic-induced renal damage in rats. *J Infect Dis* 126:593-600, 1972
9. Flandre O, Damon M: Experimental study of the nephrotoxicity of gentamicin in rats. *Gentamicin, First International Symposium*. Basel, Schwabe and Co., 1967, pp 47-61
10. Kosek JC, Masse RI, Cousins MJ: Nephrotoxicity of gentamicin. *Lab Invest* 30:48-57, 1974
11. Luft JH: Improvements in epoxy resin embedding methods. *J Biophys Biochem Cytol* 9:409-414, 1961
12. Reynolds ES: The use of lead citrate at high pH as an electron-opaque stain in electron microscopy. *J Cell Biol* 17:208-212, 1963
13. Rouiller C: General anatomy and histology of the kidney. *The Kidney, Vol I, Morphology, Biochemistry, Physiology*. Edited by C Rouiller, AF Muller. New York, Academic Press, 1969, pp 61-156
14. Ericsson JLE, Trump BF: Electron microscopy of the uriniferous tubules.<sup>13</sup> pp 351-447
15. Kempczinski RF, Caulfield JB: A light and electron microscopic study of renal tubular regeneration. *Nephron* 5:249-264, 1968
16. Ormos J, Elemér G, Csapó Z: Ultrastructure of the proximal convoluted tubules during repair following hormonally induced necrosis in rat kidney. *Virchows Arch [Zellpathol]* 13:1-13, 1973
17. Cuppage FE, Tate A: Repair of the nephron following injury with mercuric chloride. *Am J Pathol* 51:405-429, 1967
18. Oliver J: The histogenesis of chronic uranium nephritis with especial reference to epithelial regeneration. *J Exp Med* 21:425-451, 1915
19. Oliver J: Correlations of structure and function and mechanisms of recovery in acute tubular necrosis. *Am J Med* 15:535-557, 1953
20. Siegel FL, Bulgar RE: Scanning and transmission electron microscopy of mercuric chloride-induced acute tubular necrosis in rat kidney. *Virchows Arch [Zellpathol]* 18:243-262, 1975
21. Cuppage FE, Chiga M: Nuclear and mitochondrial DNA synthesis in regeneration following acute tubular necrosis of the kidney. *Am J Pathol* 66:62A, 1972 (Abstr)
22. Alouis MA, Quirke PJ: Acute tubular necrosis (ATN): Morphology of healing. *Am J Pathol* 66:63a, 1972 (Abstr)
23. Ericsson JLE: Studies on induced cellular autophagy. I. Electron microscopy of cells with *in vivo* labelled lysosomes. *Exp Cell Res* 55:95-106, 1969
24. Ericsson JLE: Mechanism of cellular autophagy. *Lysosomes in Biology and Pathology, Vol 2*. Edited by JT Dingle, HB Fell. Amsterdam, North-Holland Publishing Co., 1969, pp 345-394
25. Hruban Z, Spargo B, Swift H, Wissler RW, Kleinfeld RG: Focal cytoplasmic degradation. *Am J Pathol* 42:657-684, 1963

26. Hruban Z, Slesers A, Hopkins E: Drug-induced and naturally occurring myeloid bodies. *Lab Invest* 27:62-70, 1972
27. Gray JE, Purmalis A, Purmalis B, Mathews J: Ultrastructural studies of the hepatic changes brought about by clindamycin and erythromycin in animals. *Toxicol Appl Pharmacol* 19:217-233, 1971
28. Bangham AD: Physical structure and behavior of lipids and lipid enzymes. *Adv Lipid Res* 1:65-104, 1963
29. Revel JP, Ito S, Fawcett DW: Electron micrographs of myelin figures of phospholipide simulating intracellular membranes. *J Biophys Biochem Cytol* 4:495-498, 1958
30. Hahn FE, Sarre SG: Mechanism of action of gentamicin. *J Infect Dis* 119:364-369, 1969
31. Fowler BA, Brown HW, Lucier GW, Beard ME: Mercury uptake by renal lysosomes of rats ingesting methyl mercury hydroxide: Ultrastructural observations and energy dispersive x-ray analysis. *Arch Pathol* 98:297-301, 1974

### **Acknowledgments**

We wish to express our gratitude to Drs. Robert E. Brooks and Richard D. Moore for their expert technical and editorial assistance.

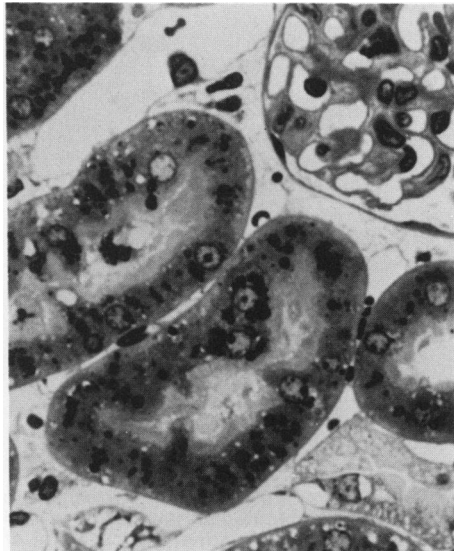
*[Illustrations follow]*



1



2



3

**Figure 1**—Electron micrograph of a proximal tubule from a control animal ( $\times 14,400$ ). **Figure 2**—Proximal convoluted tubules from a control animal (1- $\mu$  section of Araldite-embedded tissue). Cytosomes appear as scattered small dark round inclusions in epithelial cells. (Toluidine blue,  $\times 384$ ) **Figure 3**—Proximal tubules from an animal receiving gentamicin for 7 days (1- $\mu$  section of Araldite-embedded tissue). Epithelial cells contain small clear vacuoles and numerous enlarged, dark cytosomes. Collections of cytosomes are apparent within the luminal debris in one tubule. (Toluidine blue,  $\times 480$ )

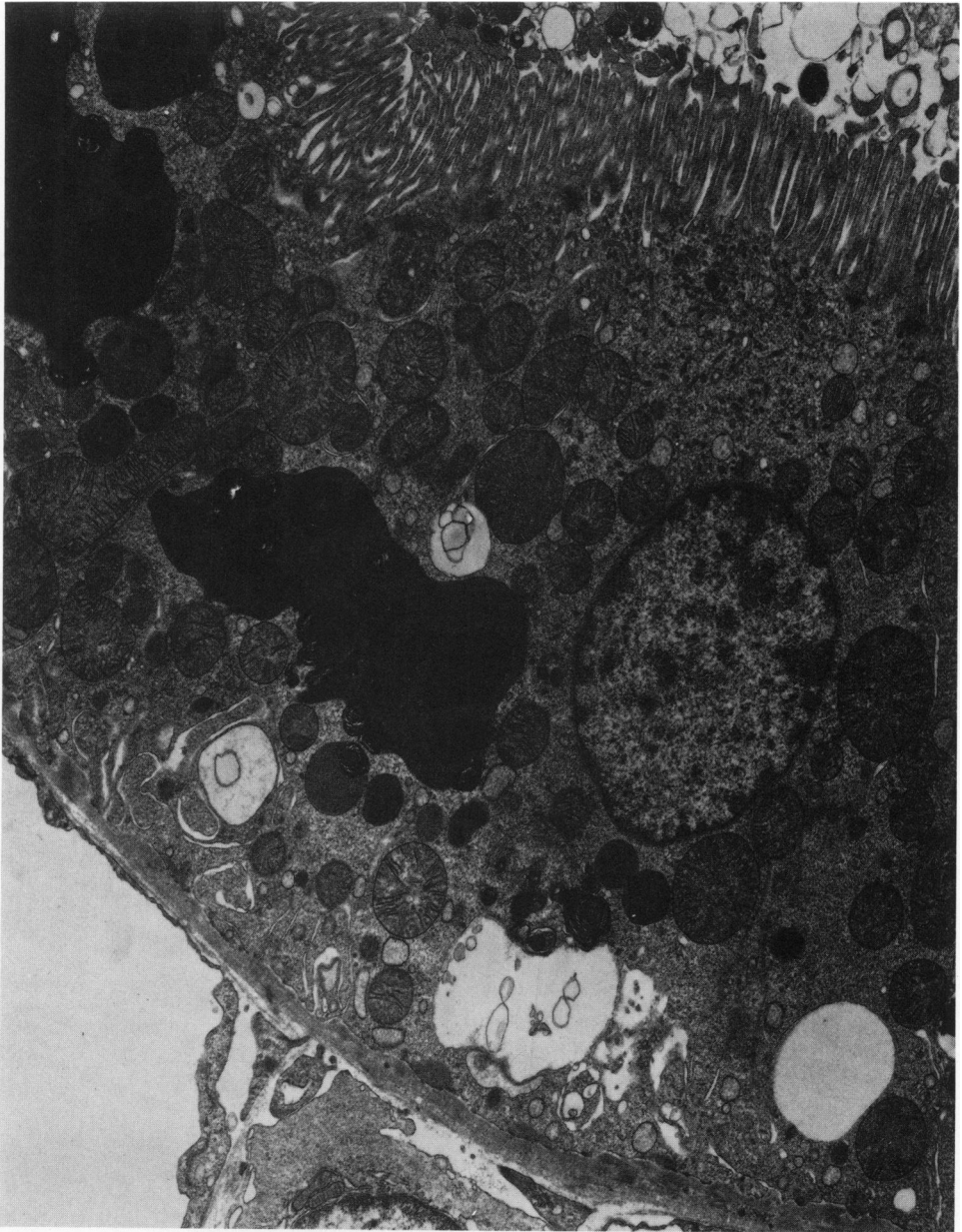


**Figure 4**—Electron micrograph of a proximal tubule after 7 days of gentamicin administration. Large irregular cytosomes contain numerous myeloid bodies. Myeloid bodies also appear free in the tubular lumen. Mitochondria and cisternae of rough endoplasmic reticulum are swollen. Large vacuoles are present near the base of the cell ( $\times 8800$ )

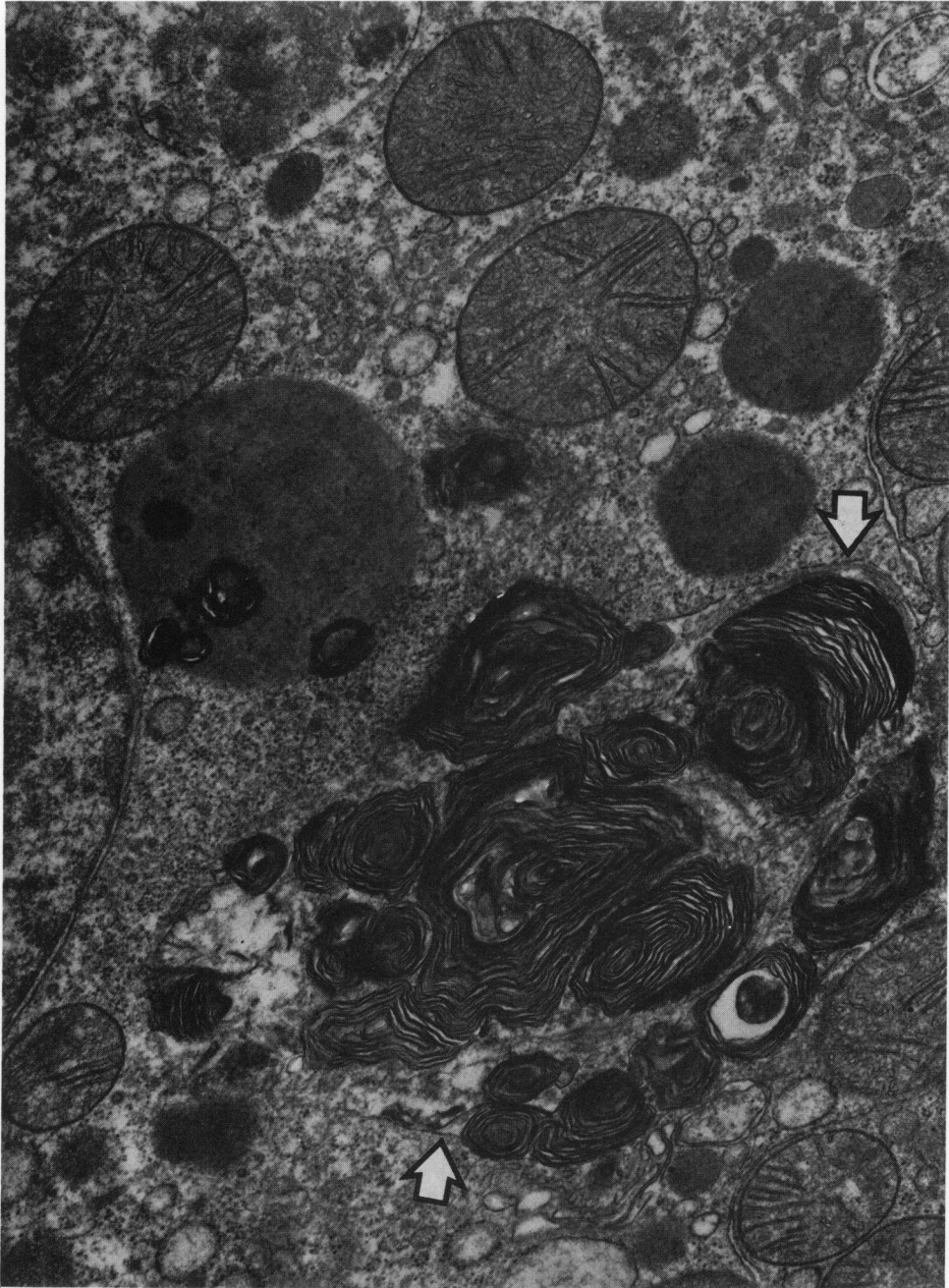


**Figure 5**—Electron micrograph of proximal tubule epithelial cell after 7 days of gentamicin. Multicentric and unicentric myeloid bodies lie free in the cytoplasm. Membranous segments at the edges of collection (*arrows*) may be remnants of lysosomal membrane. (  $\times 24,000$  )

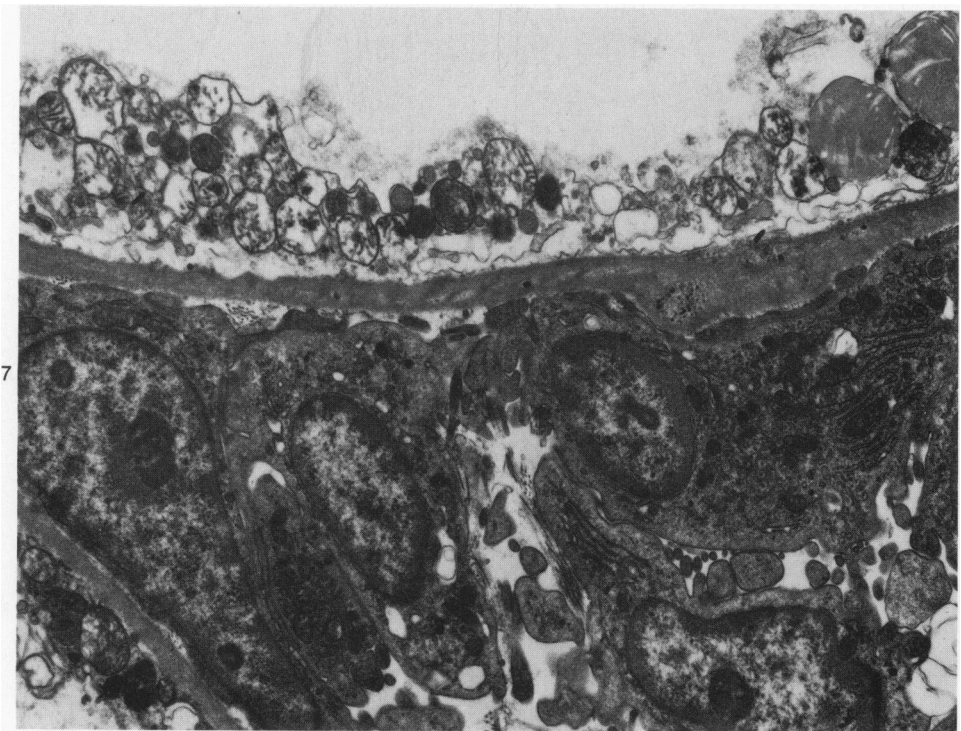
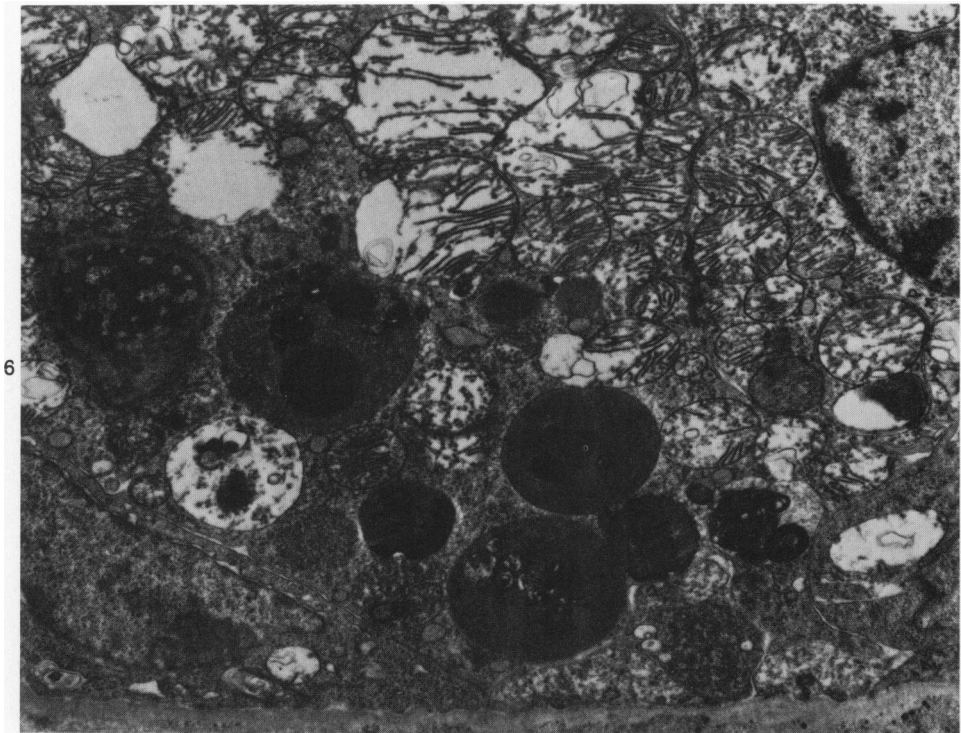


**Figure 6**—Electron micrograph of proximal tubule epithelial cell after 10 days of gentamicin. Mitochondria are greatly swollen, some showing disruption of membranes and loss of matrix. The cytoplasm is vacuolated, coarse and poorly defined. (× 8800) **Figure 7**—Electron micrograph of proximal tubule after 10 days of gentamicin. The tubular basement membrane is devoid of epithelium and cytoplasmic debris partially fills the lumen. Numerous mononuclear cells, probably histiocytes, are present in the interstitium. Granular material is trapped between layers of the basement membrane. (× 8800)



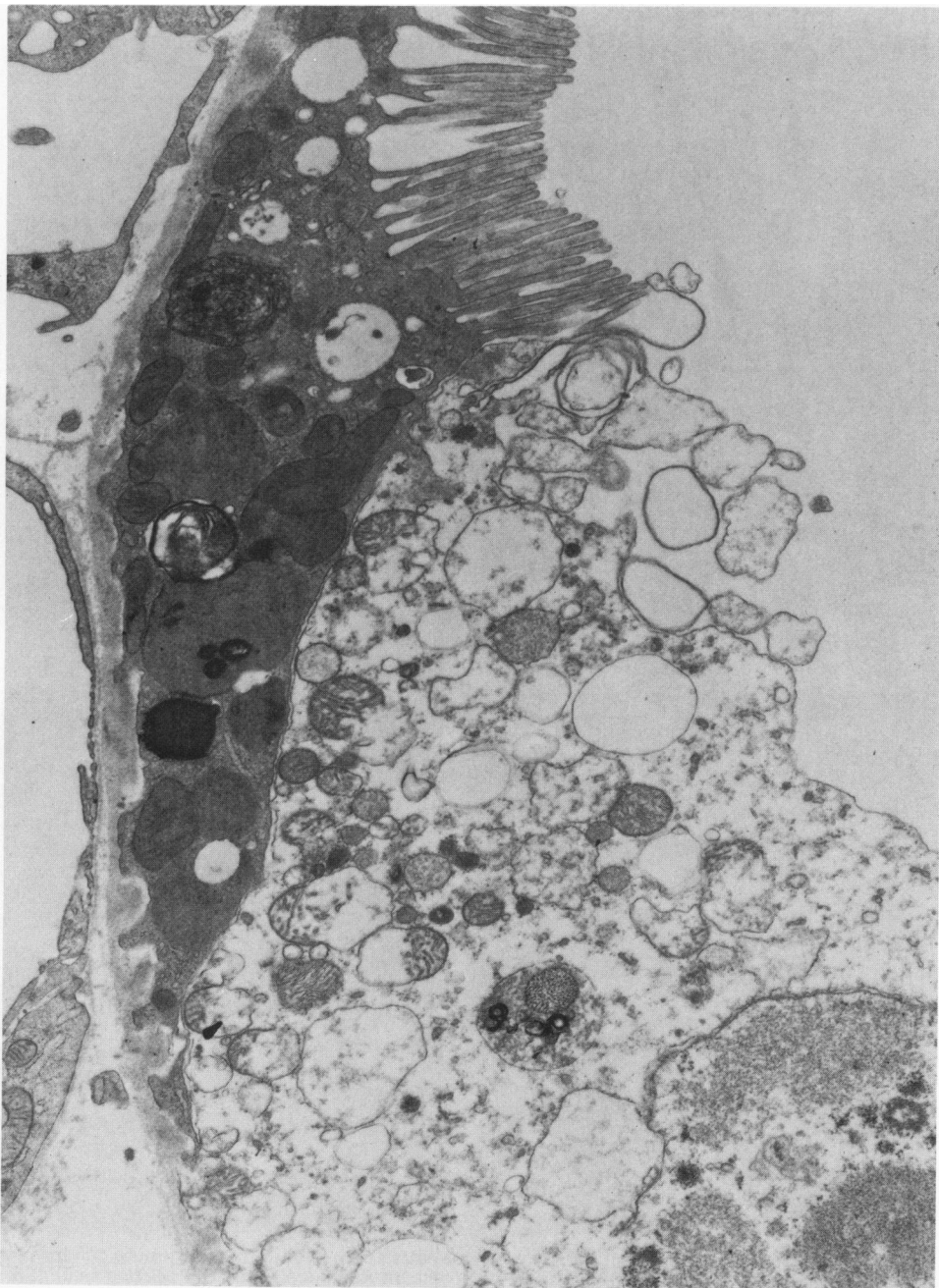


**Figure 8**—Electron micrograph of a proximal tubule after 10 days of gentamicin. A residual epithelial cell appears to be extending a narrow wedge of cytoplasm between an adjacent degenerating cell and the basement membrane. There are no tight junctions between the two cells. The residual cell has well developed microvilli, apical vesicles and several cytosomes. It has no basal infoldings. (  $\times 14,400$  )

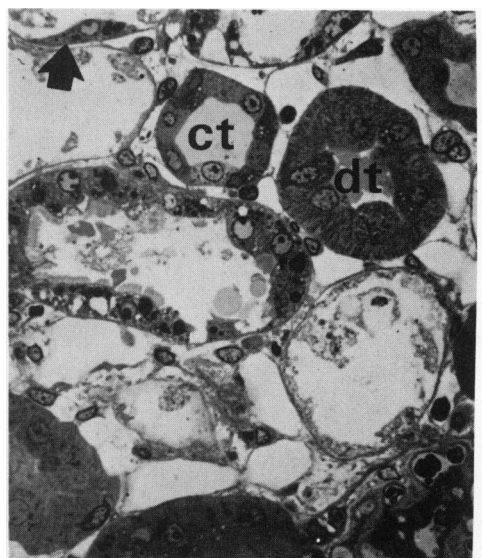
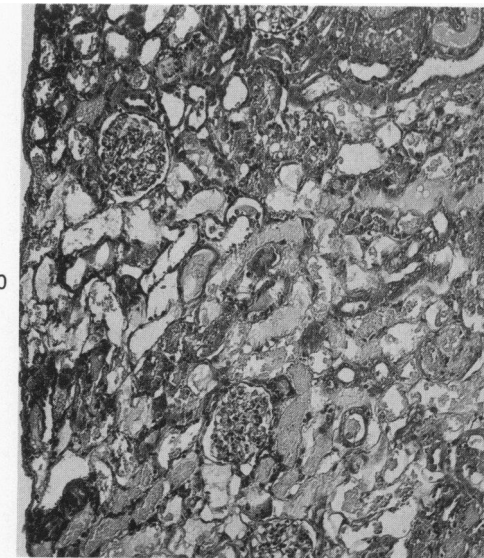
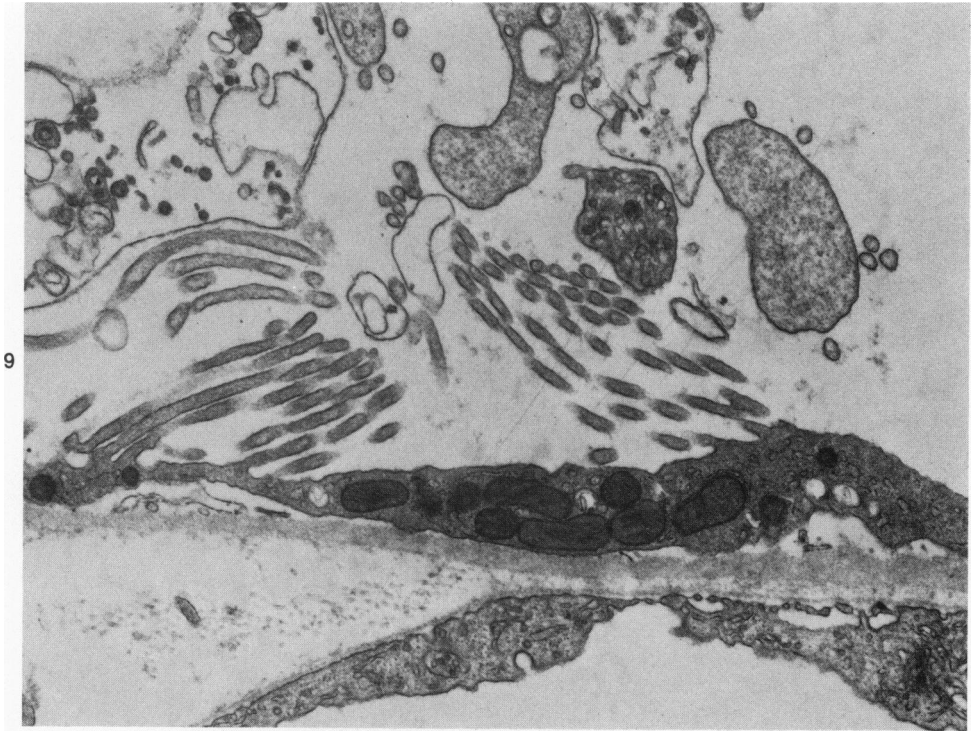


**Figure 9**—Electron micrograph of an extremely attenuated residual proximal tubule cell from an animal treated with gentamicin for 10 days. Microvilli are well developed. The cell has an undulating basal membrane which contacts the basement membrane at intervals. ( $\times 19,600$ ) **Figure 10**—Renal cortex after 10 days of gentamicin. Many proximal tubules are devoid of epithelium. Some tubules, both proximal and distal, are filled with amorphous debris while others have cleared. (H&E,  $\times 90$ ) **Figure 11**—Renal cortex after 10 days of gentamicin ( $1\text{-}\mu$  section of Araldite-embedded tissue). Proximal tubules show varying stages of epithelial cell damage and desquamation. The basement membranes of several tubules are denuded. A solitary residual cell is flattened against the basement membrane in one tubule (*arrow*). A distal tubule (*dt*) and cortical collecting tubule (*ct*) show little evidence of injury. (Toluidine blue,  $\times 360$ )

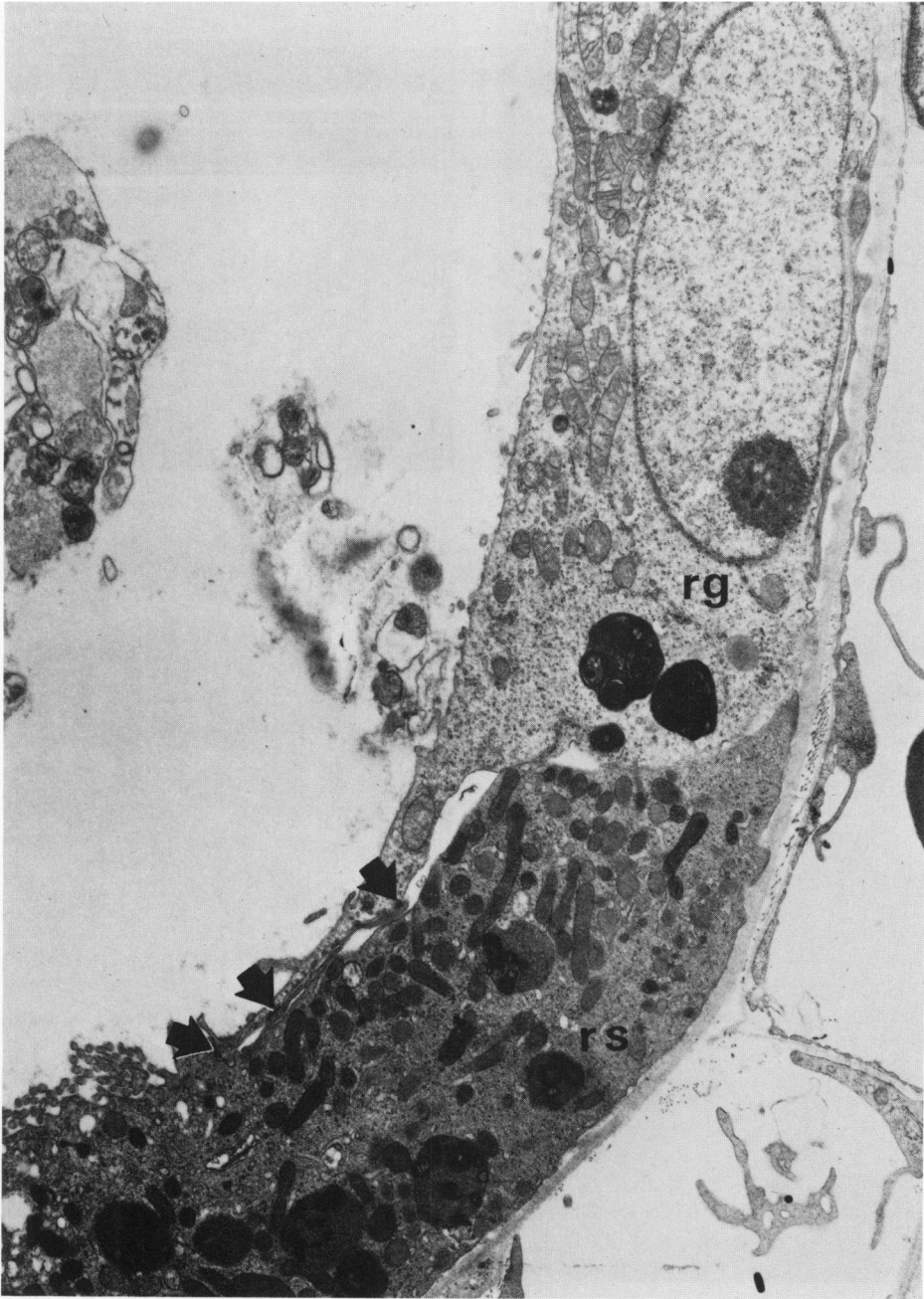


**Figure 12**—Electron micrograph of a proximal tubule after 10 days of gentamicin. Partially flattened regenerating and residual cells are bound by tight junctions (*arrows*). The regenerating cell (*rg*) has rudimentary microvilli, relatively few organelles, and ribosome-rich, loosely arranged cytoplasm. The residual cell (*rs*) has long delicate microvilli, dense cytoplasm, and more numerous and varied organelles. Both cells have myeloid body-containing cytosomes. The lumen contains cytoplasmic debris. ( $\times 8800$ )

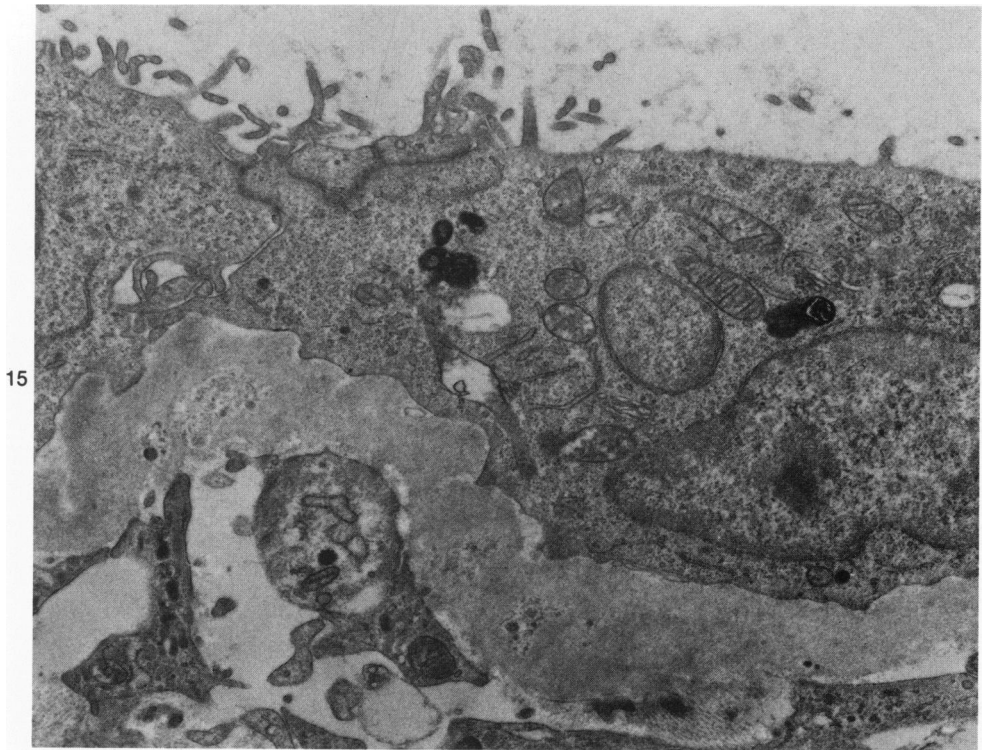
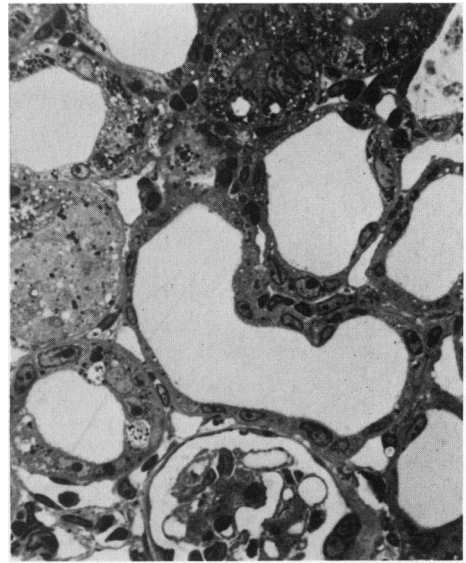
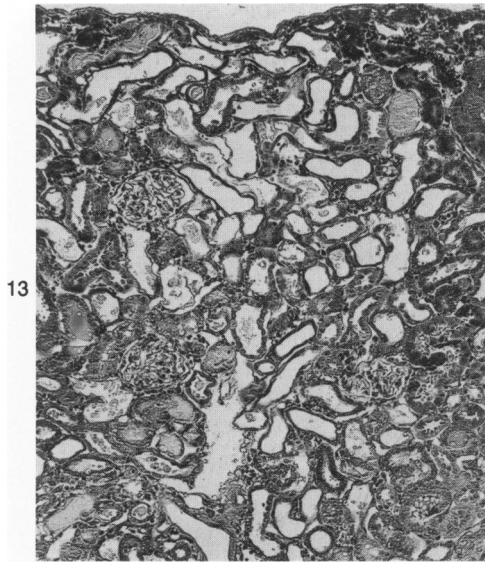
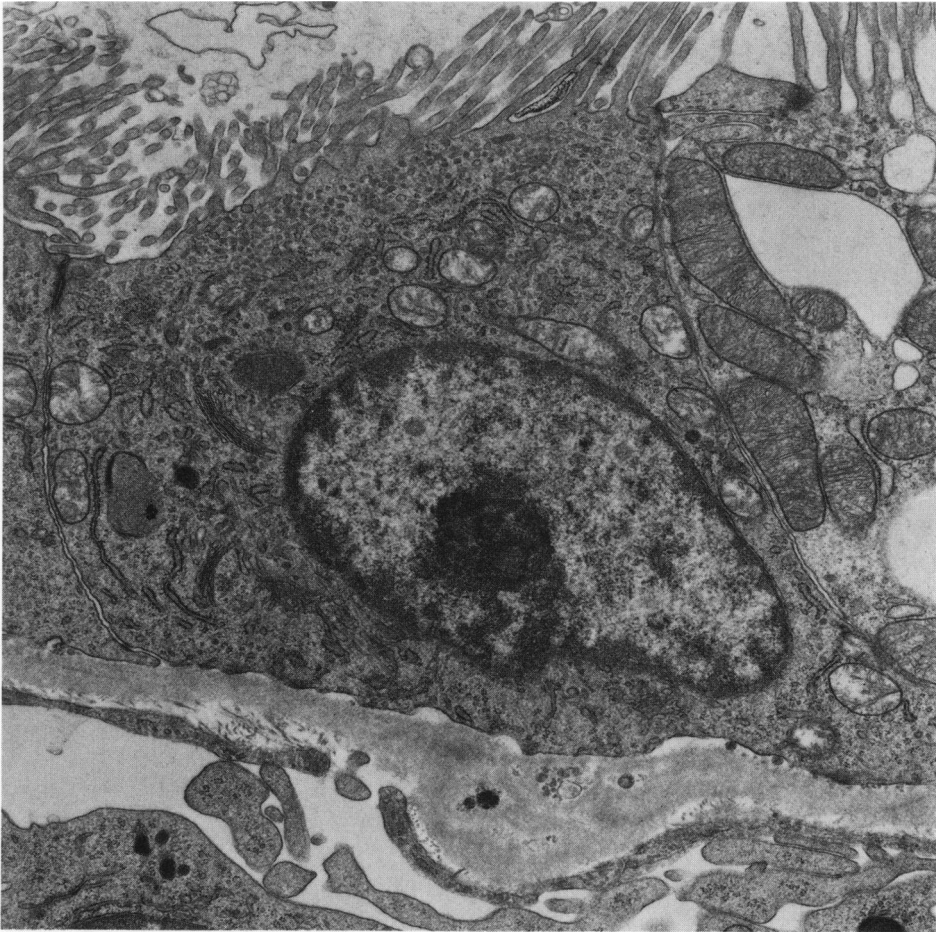
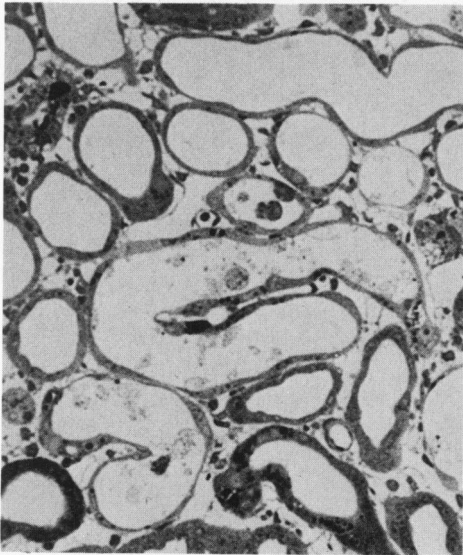


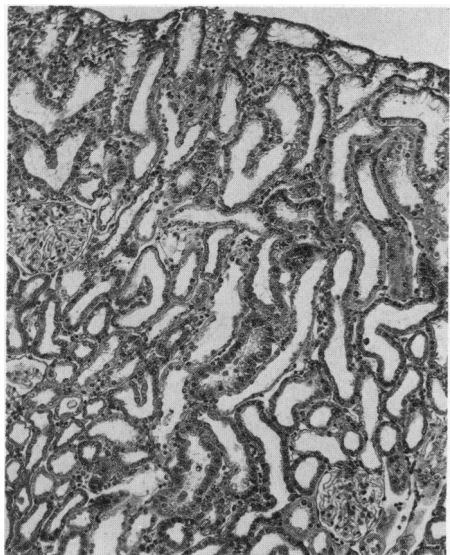
**Figure 13**—Renal cortex after 12 days of gentamicin. All but a few proximal tubules have been markedly altered. Some tubules have no epithelium, while many others are lined by squamoid, darkly staining regenerating cells. Most lumina are cleared of debris. (H&E,  $\times 90$ ) **Figure 14**—Renal cortex after 14 days of gentamicin (1- $\mu$  section of Araldite-embedded tissue). Most proximal tubules are lined by low regenerating epithelial cells with very short microvilli and small dark cytosomes. One tubule is filled with granular debris. (Toluidine blue,  $\times 360$ ) **Figure 15**—Electron micrograph of a proximal tubule after 14 days of gentamicin. These regenerating cells have microvilli which are short and widely separated. The cytoplasm contains numerous ribosomes and scattered small myeloid bodies. The cells interdigitate, and there is a broad tight junction. The basement membrane is thickened and wrinkled and contains granular debris. ( $\times 14,400$ )



16



17



18

**Figure 16**—Electron micrograph of a proximal tubule cell after 10 days of gentamicin and 2 days of recovery. Probably a residual cell, it has regained most of its normal height and ultrastructure but lacks basal infoldings. The basement membrane is focally thickened and contains granular debris. ( $\times 14,400$ ) **Figure 17**—Renal cortex after 10 days of gentamicin and 3 days of recovery (1- $\mu$  section of Araldite-embedded tissue). Proximal tubules are lined by squamoid, sometimes almost imperceptible regenerating cells. Tubules are generally cleared of debris. (Toluidine blue,  $\times 200$ ) **Figure 18**—Renal cortex after 10 days of gentamicin and 7 days of recovery. Proximal tubules are entirely relined by epithelium having appearances comparable to those of controls. (H&E,  $\times 90$ )

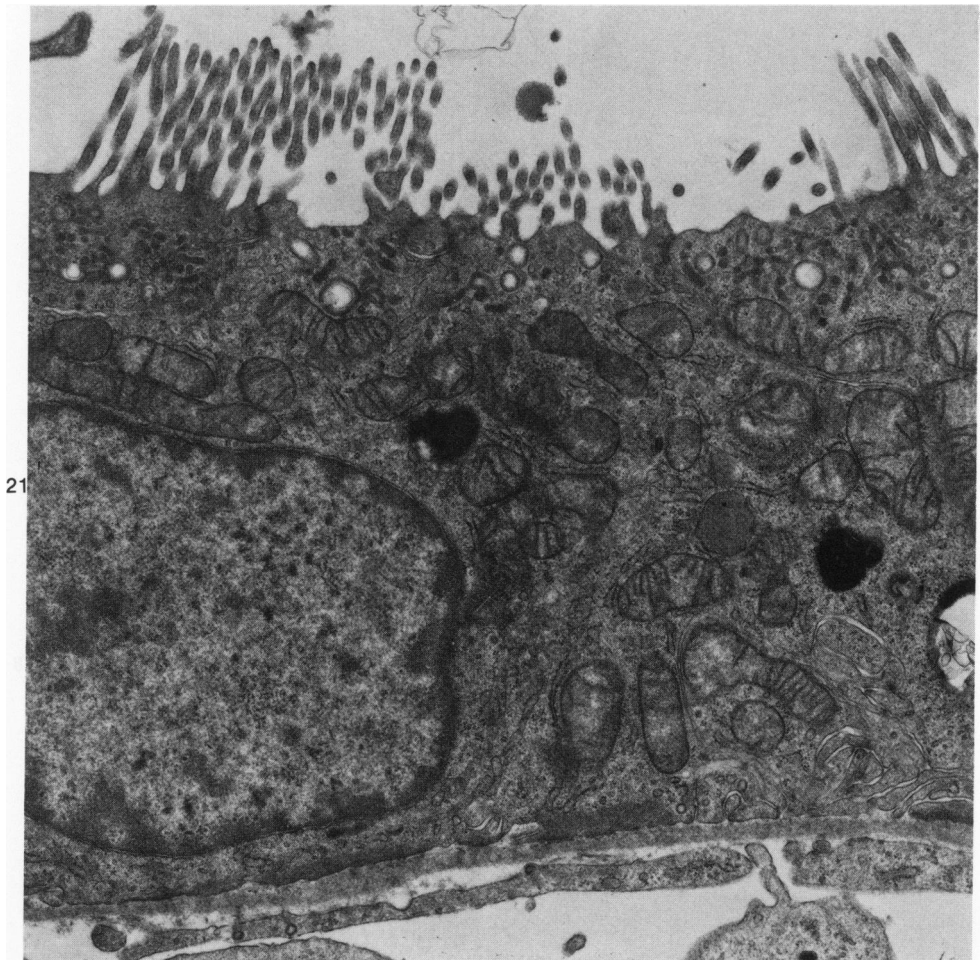
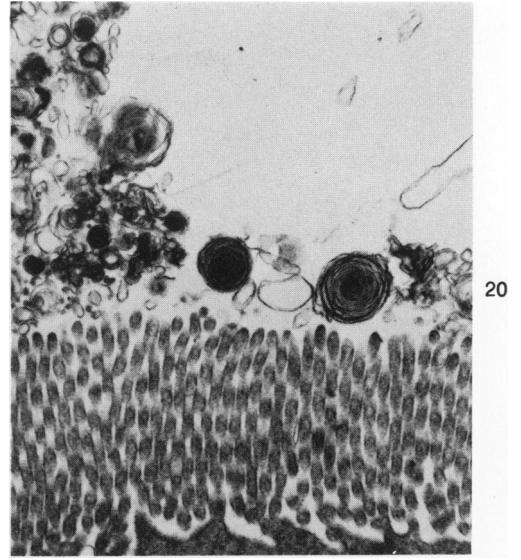
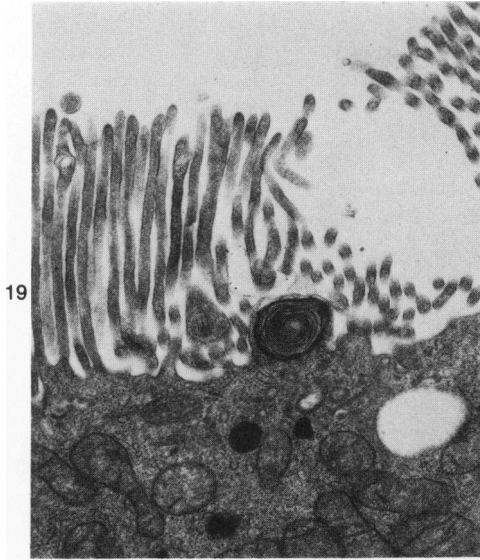
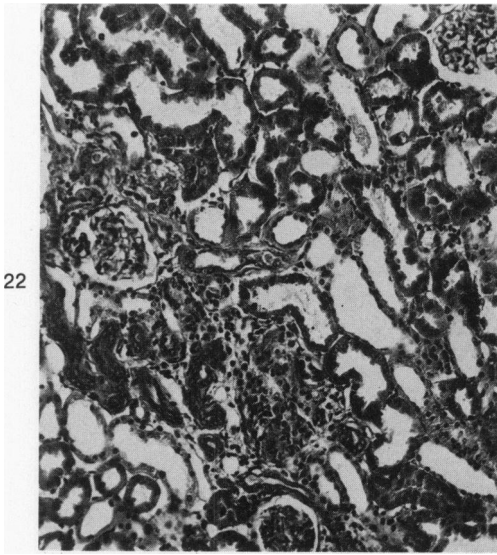
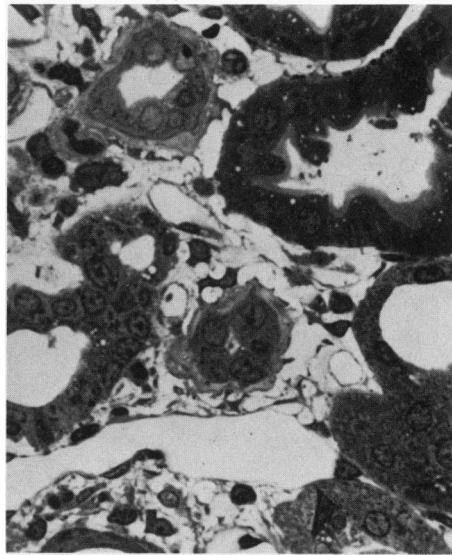


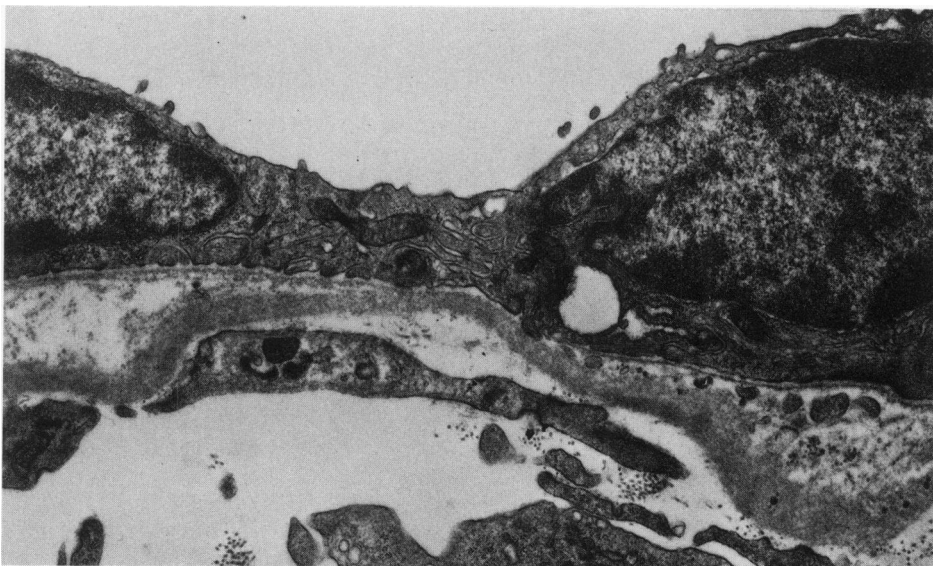
**Figure 19**—Electron micrograph of a proximal tubular epithelial cell after 10 days of gentamicin and 7 days of recovery. A myeloid body is apparently being extruded into the tubular lumen. ( $\times 14,400$ ) **Figure 20**—Electron micrograph of proximal tubular epithelial cell and lumen after 10 days of gentamicin and 7 days of recovery. Luminal debris consists largely of unicentric myeloid bodies. ( $\times 14,400$ ) **Figure 21**—Electron micrograph of a proximal tubular epithelial cell after 10 days of gentamicin and 7 days of recovery. The cell structure is comparable to controls. Basal infoldings are relatively short and simple. Smudgy dense structures are probably residual bodies. ( $\times 14,400$ )



22



23



24

**Figure 22**—Renal cortex after 10 days of gentamicin and 31 days of recovery. A small focus of compressed atrophic tubules, interstitial fibrosis, and mononuclear inflammatory cells (H&E,  $\times 110$ ) **Figure 23**—Renal cortex after 10 days of gentamicin and 31 days of recovery ( $1\text{-}\mu$  section of Araldite-embedded tissue). These two small atrophic proximal tubules have markedly thickened, irregular basement membranes. The interstitium is edematous and contains increased numbers of fibroblasts and mononuclear inflammatory cells. (Toluidine blue,  $\times 425$ ) **Figure 24**—Electron micrograph of a proximal tubule from an animal treated with gentamicin for 10 days and allowed to recover for 31 days. By light microscopy, this atrophic proximal tubule was comparable in appearance to those in Figure 23. Maturation of the epithelial cells has been delayed or arrested. They are low and relatively undifferentiated. A new basal lamina is being formed above the old wrinkled basement membrane, trapping cellular debris. ( $\times 14,400$ )

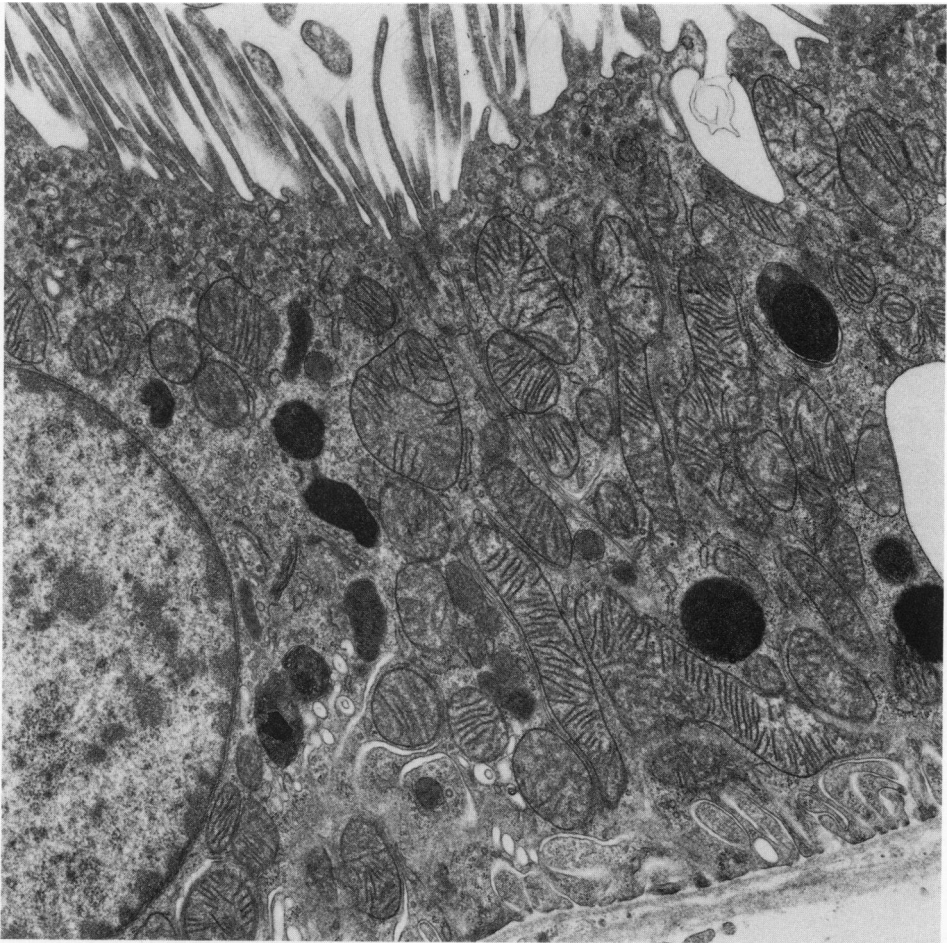


**Figure 25**—Electron micrograph of a proximal tubule cell after 10 days of gentamicin and 31 days of recovery. The cell ultrastructure is comparable to that of controls. ( $\times 14,400$ )